Electrodeposition and Characterization of Co-Mo Alloy Coatings Using Gelatin as the Additive

Yathish Rai T., A. Chitharanjan Hegde*
Department of Chemistry, Electrochemistry Lab,
National Institute of Technology Karnataka, Surathkal, Mangalore, 575025.
*Correspondence: acrhegde@gmail.com, contact: +91-9980360242

Abstract: Here, we report the electrodeposition of smooth and uniform Co-Mo alloy coating on copper from a chloride-citrate bath, using gelatin as the additive. Bath composition and operating variables were set by the conventional Hull cell method. Effects of current density on surface morphology, phase structure, and Mo content of the alloy coatings were investigated, using SEM, XRD, and EDS techniques. EDS analysis showed that in the experimented range of current density (2.0 A dm^{-2} - 6.0 A dm^{-2}), a slight decrease of Co and Mo content of the alloys was found. The compositional data of electroplated Co-Mo alloy coatings revealed that under experimented conditions, the bath follows a mixed type of co-deposition of both anomalous and induced types of co-deposition. The constancy of the phase angle of all Co-Mo Alloy coatings, deposited at different current densities confirmed the formation of solid solution of Co and Mo. The experimental study demonstrated that among Co-Mo alloy coatings, the one corresponding to 2.0 A dm^{-2} is the most corrosion resistant. The highest corrosion protection of Co-Mo alloy coatings corresponding to 2.0 A dm^{-2} was found to be more due to high wt. % of Co and lesser cracks found in the deposit. The least corrosion rate of Co-Mo alloy corresponding to 6.0 A dm^{-2} is attributed to the inhibition effect of corrosion product, formed on the surface demonstrated by the cyclic polarization study. The composition, microstructure, and corrosion resistance of Co-Mo alloy coatings were found to be the function of current density employed for deposition, supported by SEM, XRD, and EDS studies. The experimental results are discussed in the light of observed facts.

Keywords: Co-Mo alloy, corrosion study, cyclic polarization, SEM, EDS, XRD

1. Introduction

Molybdenum alloys with iron group elements (e.g., Ni, Co, Fe) represent valuable engineering materials with wide applications due to their corrosion, wear, and thermal resistances and are considered to be suitable catalytic electrodes for hydrogen evolution reaction[1–10]. Extensive study on electrodeposition of Ni-Mo and Co-Mo alloys has been done in recent years due to health and environmental concerns in the automotive or decorative plating industries. Co-Mo alloy coating is considered to be an environmentally benign alternative to chromium coatings and hence it has practical significance for industry[11]. Codeposition of Mo with iron group metals is induced since the complete reduction of Mo in aqueous solutions does not occur in the absence of an iron group metal[12]. Several studies have examined the anomalous electrodeposition of Ni-Mo, especially in a citrate medium, although there are fewer reports on Co-Mo or Fe-Co deposition[13,14]. A recent study on the influence of bath composition and pH on the electrochemical behavior of Co-Mo deposition revealed that the equilibria between the species in solution play an important role on electrodeposition[15]. It was found that alloy deposition occurred through different stages depending on the pH of the bath, which affected the composition of the final deposit[16]. Hence, there are several studies demonstrating the fact that bath composition and current density has significant effect on type of codeposition of Co-Mo alloy coatings and its physico-mechanical properties. Generally, the corrosion protection efficacy of alloy coatings largely depends on its homogeneity and uniformity. Therefore, to improve the uniformity and hence the corrosion protection efficacy of electrodeposited Co-Mo alloy coating, gelatin can be used as the additive.

Table 1 – Bath composition and operating parameters of the optimized Co-Mo bath

Bath composition	Concentration (g/L)	Operating Parameters
Cobalt (II) chloride hexahydrate ($CoCl_2.6H_2O$)	15.0	pH: 10.0 Temperature: 303K Anode: Graphite Cathode: Copper Current density: 2.0 - 6.0 A dm^{-2} Deposition time: 600 s
Sodium molybdate dihydrate ($Na_2MoO_4.2H_2O$)	30.0	
Trisodium citrate dihydrate ($Na_3C_6H_5O_7.2H_2O$)	30.0	
Gelatin	0.5	

The added gelatin can improve both brightness and uniformity of alloy coatings by bringing a significant change in nucleation process and grain refining action, during deposition[17]. A new chloride-citrate bath of Co-Mo alloy has been tried to explore using gelatin as the additive. Bath composition and operating variables have been optimized for best performance of thin coatings using standard Hull cell method. To ensure the good adhesion of electrodeposited coatings, copper substrates were properly cleaned, following the standard method. Copper panels of 2.5 ×3.0 cm^2 area were pre-treated by mechanical polishing, using emery coated mops of gradually decreasing grit sizes. The mirror polished specimens were then degreased with trichloroethylene (TCE). Then, the plates were electro-cleaned cathodically for 2 minutes, and then anodically for 30 seconds. Later, specimens were washed in running water, rinsed in distilled water, and then immediately taken for deposition. The influence of current density on corrosion protection efficacy of Co-Mo alloy coatings were studied. The deposition current density has been optimized considering the best corrosion protection ability of Co-Mo alloy coatings. The type of codeposition (the bath follows) was analysed on the basis of metal contents in bath and electrodeposit. Corrosion stability of alloy coatings, and factors responsible for it are discussed. The composition, phase structure and surface morphology of alloy coatings were analysed using, respectively EDS, XRD and SEM techniques, and results are discussed.

2. Materials and methods

2.1 Optimization of Co-Mo bath

A simple and new chloride-citrate bath of Co-Mo alloy containing cobalt (II) chloride ($CoCl_2.6H_2O$), trisodium citrate ($Na_3C_6H_5O_7.2H_2O$), and sodium molybdate ($Na_2MoO_4.2H_2O$) has been formulated, using gelatin as the additive. All reagents except gelatin, were dissolved in double distilled water, individually and then mixed and stirred well for complete dissolution. Gelatin, the primary additive was dissolved first in cold water, and then heated to get a clear solution. A clear solution of gelatin was added to the bath to maintain the overall concentration of the bath. The standard Hull cell method was employed for optimization of bath composition and plating variables[17] to develop bright, smooth, and uniform Co-Mo alloy coatings. The composition and operating variables of Co-Mo bath, which are fixed through the Hull cell are given in Table 1.

The electrodeposition of Co-Mo alloy coatings was performed in a 200mL capacity cell (made of polyvinyl chloride material) using a DC Power Analyzer (Agilent N6705C, USA). To ensure the good adhesion of alloy coatings, the substrate was properly cleaned, following the standard method. Copper panels of 7.5 cm × 3.0 cm × 0.2 cm dimensions were pre-treated by mechanical polishing, using emery coated mops of gradually decreasing grit sizes. The mirror polished specimens

were then degreased with trichloroethylene (TCE). Then, the plates were electro-cleaned cathodically for 2 minutes, and then anodically for 30 seconds. Later, specimens were washed in running water, rinsed in distilled water, and then immediately taken for deposition, keeping 3.0 × 3.0 cm^2 active surface area, by covering the remaining surface by cellophane tape. A graphite bar, having the same active surface area, was used as an anode. After deposition, the coatings were rinsed with distilled water several times, dried in hot air, and then desiccated until further testing. All electrodepositions were carried out at pH 10.0 (adjusted by using either HCl or NH_4OH) for a time period of 600 s. The deposition condition was kept constant for all the coatings, for comparison of their properties and performances.

Further, the corrosion performances of developed coatings were evaluated in a 3.5% NaCl solution. The corrosion study was carried out using a three-electrode cell, where Co-Mo alloy coated copper substrate was used as the working electrode, the Pt electrode serves the role of the counter electrode and the saturated calomel electrode was used as the reference electrode. The electrochemical techniques such as potentiodynamic polarization and electrochemical impedance spectroscopy (EIS) were employed for corrosion behavioral study of developed alloy coatings, using a potentiostat/ galvanostat (Biologic SP-150). After desiccator drying, the coatings were subjected to an electrochemical corrosion test, and corrosion rates were measured by Tafel's extrapolation method, in a potential window of ± 250 mV from the open circuit potential, at a scan rate of 1mV/s. The EIS study was carried out using 10 mV perturbing AC voltage, in a frequency range of 100 kHz to10 mHz, and the corresponding Nyquist plots were analyzed in terms of their polarization resistance (R_p) values. All Co-Mo alloy coatings were subjected to an EIS study prior to potentiodynamic polarization analysis. The changes in the surface structure and the composition of Co-Mo alloy coatings with current density were analyzed using scanning electron microscopy (SEM), a device of Zeiss Ultra 55, Germany, and energy dispersive X-ray spectroscopy (EDS) techniques (Oxford EDS, X-act), respectively. The composition-dependent crystal structures of Co-Mo alloy coatings were characterized by X-ray diffraction (XRD), (Rigaku, Miniflex 600), with CuK_α radiation, λ = 1.5418 Å, as the X-ray source. The corrosion product responsible for better corrosion stability of Co-Mo alloy coating under optimal conditions was analyzed using the cyclic polarization technique by reversing the direction of anodic polarization.

3. Results and discussion

3.1 Compositional analysis

It is a well-known fact that the corrosion protection efficacy of electrodeposited alloy coatings depends mainly on their composition and surface microstructure. Accordingly, composition analysis of

Table 2. Corrosion parameters of Co-Mo alloy coatings deposited at different current densities with wt. % metal contents in the deposit and in the bath

Current density (A dm^{-2})	wt. % of Co	wt.% of Mo	Thickness of coating (μm)	$-E_{corr}$ (mV vs. SCE)	i_{corr} (μA cm^{-2})	CR $\times 10^{-2}$ ($mmyr^{-1}$)
2.0	68.6	31.4	5.0	497.8	22.39	18.09
3.0	66.5	33.5	7.2	509.5	28.41	23.40
4.0	61.7	38.3	9.0	532.2	32.44	25.31
5.0	60.9	39.1	12.5	532.9	39.28	30.44
6.0	60.2	39.8	15.4	511.8	44.99	34.68
Wt. % of metal content in the bath						
	33.3	66.6				

Co-Mo alloy coatings, corresponding to different current densities was carried out, using EDS technique and are reported in Table 2.

The variation of metals (Co and Mo) content in the deposit with current density is shown graphically in Fig. 1. The composition reference line (CRL) corresponds to the wt. % of Co and Mo in the bath, based on the weight of salt taken is shown by horizontal perforated lines. From the composition data (Table 2) it may be noted that wt. % of Co (noble metal) in the deposit slightly decreases with current density, and that of Mo increases with current density. In addition to this, it may be pointed out that wt. % of Co and Mo in the deposit are almost on par with that in the bath. Generally, the effect of operating variables on the composition of the alloy deposit does not follow any definite rules. In many alloy plating processes, an increase in current density causes the content of the more noble metal in the deposit to decrease; and an increase in the temperature, or the agitation of the bath causes the content of the more noble metal to increase. These trends are followed consistently by the regular type of alloy plating systems, and fairly frequently by the irregular type of alloy plating systems, eventhough there are number of exceptions to this general trend. Thickness of electrodeposited Co-Mo alloy coatings were measured using digital thickness tester (Coat Measure M&C), and it was further verified from Faraday's law and they are found to be in the range of 5 – 15 μm as shown in Table 1.

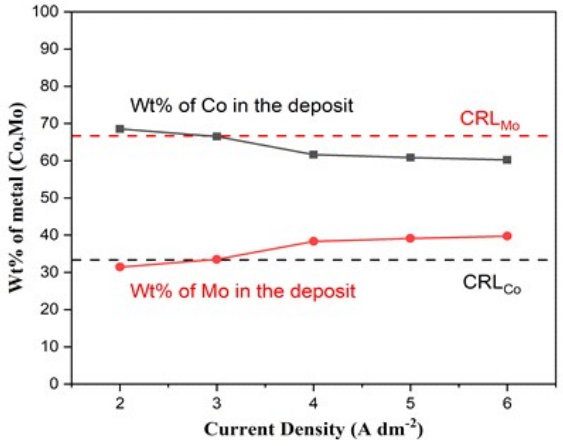


Fig. 1 - Dependency of Wt % of Co and Mo in the deposit with current density

It may be recalled that even though under general conditions, Co-Mo alloy follows an induced type of co-deposition by featuring a negligible change of reluctant metal (Mo) content in the deposit with current density, there are many exceptions to this trend of alloy composition with current density[12]. In other words, the effect of current density on the anomalous and the induced types of co-deposition are not consistent enough to be predicted. Therefore, from the composition data of Co-Mo alloy coatings of the present study, it may be proposed that the present bath follows a mixed type of co-deposition by following the anomalous type of co-deposition (decrease of cobalt content with the increase of current density) and induced type of co-deposition (constancy of metal content with current density).

3.2 Surface Morphology

The surface morphology of developed Co-Mo alloy coatings was studied by SEM analysis, and SEM micrographs of alloy coatings corresponding to different deposition current densities were shown in Figure 2.

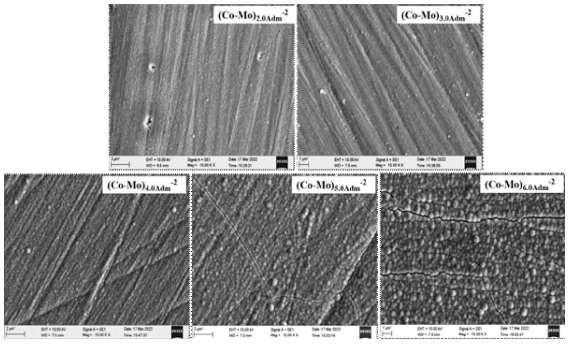


Fig. 2 - Surface morphology of Co-Mo alloy coatings corresponding to different current densities deposited from an optimal bath. The characteristic cracks having specific patterns found to grow with the increase of current density due to the liberation of H_2

It is may be seen that the morphology of alloy coatings bears close relation with the current densities used for its deposition. SEM micrographs confirmed the formation of micro-cracks at high current density and is due to the combined effect of increased Mo content and hydrogen embrittlement. It is important to note that the observed cracks of specific patterns are the characteristic feature of binary alloys of Fe-group metals with Mo and P. The characteristic

cracks having specific patterns were found to grow with the increase of current density. The cracks of Co-Mo alloy coatings may be attributed to hydrogen embrittlement, affected due to simultaneous liberation of H_2 on the cathode during deposition. Accordingly, as the current density is increased, the liberation of H_2 on cathode surface has also increased. This increase of with in liberation of H_2 on the cathode, is due to an increase in current density made to increase the depth and width of cracks, and is evidenced by SEM micrographs of coatings, shown in Fig. 2. The formation of cracks on the surface of the cathode may also be attributed to low hydrogen overvoltage of Mo. Hydrogen gets adsorbed on the surface of the electrode, and it ultimately leads to the formation of micro-cracks in the deposit. A crack-free, compact deposits were obtained at lower current densities, due to its lower Mo content.

3.3 X-Ray Diffraction Study

The phase structure of electrodeposited Co-Mo alloy coatings was analyzed by the XRD technique, and the corresponding X-ray diffractograms are shown in Figure 3. The examination by X-ray patterns justifies that all coatings are well-crystalline. The XRD peaks observed at the same scattering angles corresponding to coatings of different current density indicates the formation of solid solutions of Co and Mo formed, regardless of the current density at which they are deposited.

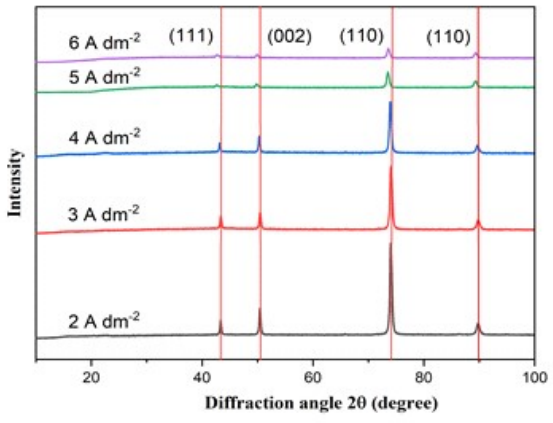


Fig. 3. XRD patterns of Co-Mo alloy coatings deposited at different current densities from an optimal bath. The constancy of phase angles of coatings corresponding to different current densities indicate the formation of a solid solution of Co with Mo.

Lattice planes (111), (002), (110), and (110) were corresponding to lattice reflections of hexagonal cubic close-packed structures. The presence of the same lattice planes in all XRD patterns obtained indicates the same crystal structure of Co-Mo deposits is formed at all deposition current densities. However, a small shift in the diffraction lines towards lower angles may be attributed to lattice distortion, due to the incorporation of Mo atoms into the Co matrix. The intensity of diffraction lines is observed to be decreased with the increase of current densities as shown in Figure 3. This decreased intensity of peaks with current density may be attributed to the decreased Co content of alloy coatings.

3.4 Corrosion study of Co-Mo Alloy Coatings

The aim of the present study is to understand the effect of current density on composition, and hence corrosion behavior of Co-Mo alloy coatings. The corrosion study of Co-Mo alloy coatings was accomplished using EIS and potentiodynamic polarization methods and the results are discussed below.

3.4.1 EIS study

EIS is a non-destructive technique that gives valuable information regarding the structure of the interface and various interfacial reactions taking place there[18]. It consists of studying the impedance (AC resistance) over a range of frequencies, by passing an alternating current of small amplitude, and presenting it in the form of popular Nyquist plots[19]. Here, impedance (Z) is represented as a complex number, having a real impedance part (Z') and imaginary impedance part (Z"), over a range of frequency (100 kHz to 10 mHz), and such representation is provided with provision to distinguish the contribution of polarization resistance (R_p) versus solution resistance (R_s) of a test electrode.

Accordingly, Nyquist plots of Co-Mo alloy coatings are shown in Figure 4. The interception of capacitive loops on the real axis at higher frequency corresponds to solution resistance (Rs) and at lower frequency corresponds to charge transfer resistance (R_{ct}) or polarisation resistance (R_p). The diameters of the semicircles in the Nyquist diagram represent the charge transfer resistance $R_{ct,}$ which is equivalent to polarization resistance R_p. i.e., which indicates the

resistance to undergo oxidation. Hence, from the nature of capacitive loops seen in Figure 4, it is evident that a Co-Mo alloy coating developed at 2.0 A dm^{-2} exhibits the highest R_p value, compared to that of all other coatings. This could be due to the decreased cracks and increased Co content in the deposit.

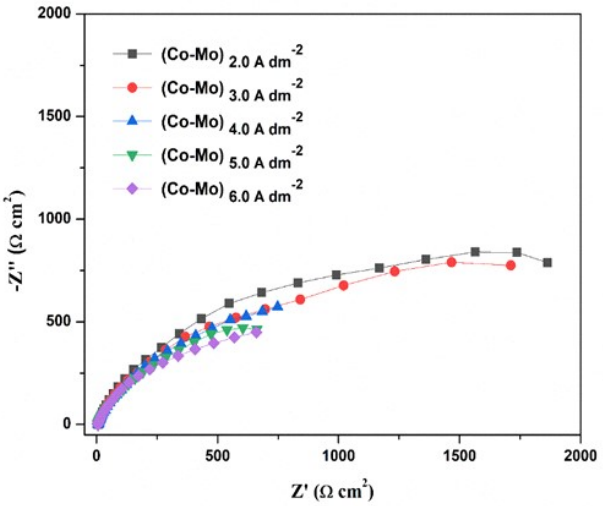


Fig. 4 - Nyquist plots of Co-Mo alloy coatings deposited at different current densities. The highest polarization resistance (R_p) of Co-Mo coating corresponding to 2.0 A dm^{-2} may be seen, compared to other coatings.

3.4.2 Potentiodynamic polarization method

After the EIS study, potentiodynamic polarization analysis of Co-Mo alloy coatings was carried out, and corresponding responses are presented in the form of Tafel plots, shown in Figure 5. The corrosion rates were evaluated by conventional Tafel extrapolation method, and their corrosion data are reported in Table 2. Tafel's plots demonstrate that the corrosion rate of coating deposited at the current density of 2.0 A dm^{-2} is the least one compared to other coatings, it is further supported by its more cathodic E_{corr} value as shown in Fig. 5.

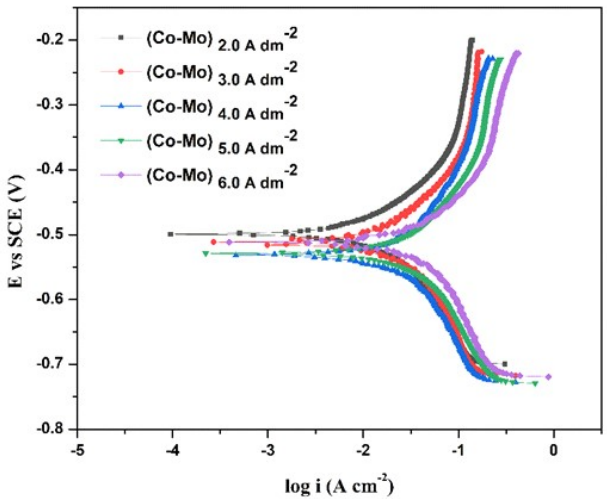


Fig. 5. Polarization behavior of Co-Mo alloy coatings deposited at different current densities. Tafel plot corresponding to Co-Mo alloy coating of 2.0 A dm^{-2} showing less i_{corr} value compared to other current density is seen

3.5 Cyclic polarization study

The reasons responsible for the highest corrosion protection of Co-Mo alloy coating at 2.0 A dm^{-2} were tried to understand by cyclic polarization method in a potential ramp from -0.650V to 0.650V, and is shown in Fig. 6. In the forward scanning, the value of current increased from negative to positive. This indicated that the oxidizing reaction of passivation film occurred with increasing potential. During backward scanning, the current followed the same path as that of forward scanning as shown in Fig. 6. It indicates that corrosion products formed do not offer any inhibitory protection against corrosion. However, the E_{corr} value corresponding to corrosion product is found to be much higher (nobler) than that of electrodeposited alloy coatings as may be seen in Figure 6. This indicates the fact that corrosion product by being nobler than coated alloy, acts as a barrier and gives better protection to the substrate.

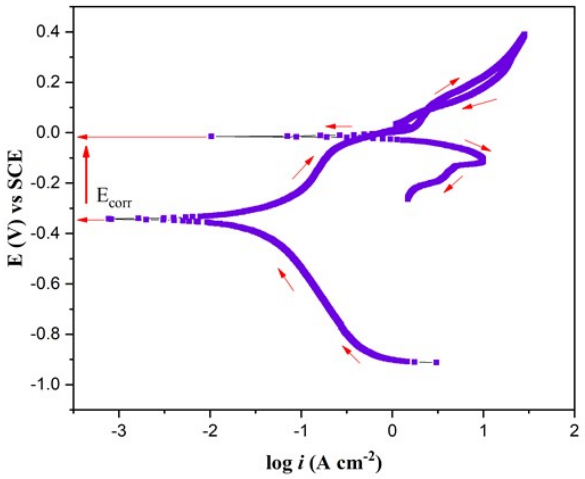


Fig. 6 - Cyclic polarization behavior of Co-Mo alloy coating deposited at 2.0 A dm^{-2}, showing an increased E_{corr} value corresponding to the corrosion product indicating that better corrosion stability is due to its barrier protection

Thus, the cyclic polarization study exemplifies that the high corrosion stability of Co-Mo alloy coating deposited at 2.0 A dm^{-2} is due to the inhibition effect of corrosion products formed on the substrate where it acts as a barrier between the metal and medium.

4. Conclusions

Electrolytic Co-Mo alloys have been deposited from a chloride-citrate bath using gelatin as the additive, and following observations were made as conclusions:

1. A new electrolytic bath has been optimized for electrodeposition of Co-Mo alloy on copper substrate by the Hull cell method, using gelatin as the brightener.

2. Bright and uniform Co-Mo alloy coatings have been developed in the current density range of 2.0 - 6.0 A dm^{-2}, and their corrosion behaviors have been studied.

3. The compositional data of electroplated alloy coatings revealed that under experimented conditions, the bath follows a mixed type of co-deposition, of both anomalous and induced type.

4. The constancy of the phase angle of all Co-Mo Alloy coatings at different current densities confirmed the formation of a solid solution of Co and Mo.

5. The experimental study demonstrated that among all coatings, Co-Mo alloy coating corresponding to 2.0 A dm^{-2} is the most corrosion resistant, and is attributed to its highest Co content and smoothness.

6. The least corrosion rate of Co-Mo alloy coating, deposited at 2.0 A dm^{-2} is ascribed to the inhibition effect of corrosion product formed on the surface, evidenced by cyclic polarization study.

7. The composition, microstructure, and corrosion resistance of Co-Mo alloy coatings were found to be the function of the current density employed for deposition, supported by SEM, XRD, and EDS studies.

Acknowledgement

Yathish Rai T is thankful to National Institute of Technology Karnataka (NITK), Surathkal, India, for providing the financial support to carry out this work in the form of Institute Research Fellowship.

References

(1) 100604972.Pdf.

(2) Pavlov, M. P.; Morozova, N. V.; Kudryavtsev, V. N. Electrodeposition of Nickel-Molybdenum Alloys from Ammonium Citrate Baths Containing Intermediate Valence Molybdenum Compounds. *Prot Met* **2007**, *43* (5), 459–464. https://doi.org/10.1134/S0033173207050074.

(3) Prioteasa, P.; Golgovici, F.; Sbircea, G.; Anicai, L.; Visan, T. Electrodeposition, Structure and Corrosion Behaviour of Ni-Mo Alloys from Citrate Aqueous Electrolyte. *REV. CHIM.* **2010**, 9.

(4) Lima-Neto, P. de; Correia, A. N.; Vaz, G. L.; Casciano, P. N. S. Morphological, Structural, Microhardness and Corrosion Characterisations of Electrodeposited Ni-Mo and Cr Coatings. *J. Braz. Chem. Soc.* **2010**, *21* (10), 1**968–1976.** https://doi.org/10.1590/S0103-50532010001000024.

(5) Han, Q.; Cui, S.; Pu, N.; Chen, J.; Liu, K.; Wei, X. A Study on Pulse Plating Amorphous Ni–Mo Alloy Coating Used as HER Cathode in Alkaline Medium. *International Journal of Hydrogen Energy* **2010**, *35* (11), 5194–5201. https://doi.org/10.1016/j.ijhydene.2010.03.093.

(6) Birry, L.; Lasia, A. Studies of the Hydrogen Evolution Reaction on Raney Nickel–Molybdenum Electrodes. *Journal of Applied Electrochemistry* **2004**, *34* (7), 735–749. https://doi.org/10.1023/B:JACH.0000031161.26544.6a.

(7) Ramesh, L.; Sheshadri, B. S.; Mayanna, S. M. Electrolytic Preparation and Characterization of Ni-Fe-Mo Alloys: Cathode Materials for Alkaline Water Electrolysis. *Int. J. Energy Res.* **1999**, *23* (10), 919–924. https://doi.org/10.1002/(SICI)1099-114X (199908) 23:10<919::AID-ER524>3.0.CO;2-D.

(8) Pellicer, E.; Gómez, E.; Vallés, E. Use of the Reverse Pulse Plating Method to Improve the Properties of Cobalt–Molybdenum Electrodeposits. *Surface and Coatings Technology* **2006**, *201* (6), 2351–2357. https://doi.org/10.1016/j.surfcoat.2006.04.011.

(9) Kublanovskii, V. S.; Yapontseva, Yu. S.; Troshchenkov, Yu. N.; Gromova, V. A. Corrosion and Magnetic Properties of Electrolytic Co-Mo Alloys. *Russ J Appl Chem* **2010**, *83* (3), 440–444. https://doi.org/10.1134/S1070427210030134.

(10) Kublanovsky, V. S.; Yapontseva, Y. S. Electrocatalytic Properties of Co-Mo Alloys Electrodeposited from a Citrate-Pyrophosphate Electrolyte. *Electrocatalysis* **2014**, *5* (4), 372–378. https://doi.org/10.1007/s12678-014-0197-y.

(11) Costovici, S.; Manea, A.-C.; Visan, T.; Anicai, L. Investigation of Ni-Mo and Co-Mo Alloys Electrodeposition Involving Choline Chloride Based Ionic Liquids. *Electrochimica Acta* **2016**, *207*, 97–111. https://doi.org/10.1016/j.electacta.2016.04.173.

(12) A. Brenner: Electrodeposition of Alloys. Principle and Practice. Academic Press, New York and London 1963. Band I: General Survey, Principles, and Alloys of Copper and of Silver. 714 S. Mit 212 Bildern Und 45 Tab. DIN A5. Preis: $ 24.-. *Berichte der Bunsengesellschaft für physikalische Chemie* **1964**, *68* (3), 309–309. https://doi.org/10.1002/bbpc.19640680319.

(13) Beltowska-Lehman, E.; Indyka, P. Kinetics of Ni–Mo Electrodeposition from Ni-Rich Citrate Baths. *Thin Solid Films* **2012**, *520* (6), **2046–2051.** https://doi.org/10.1016/j.tsf.2011.10.024.

(14) Podlaha, E. J.; Landolt, D. Induced Codeposition: III. Molybdenum Alloys with Nickel, Cobalt, and Iron. *J. Electrochem. Soc.* **1997**, *144* (5), **1672–1680.** https://doi.org/10.1149/1.1837658.

(15) Gymez, E.; Pellicer, E.; Alcobé, X.; Vallés, E. Properties of Co-Mo Coatings Obtained by Electrodeposition at PH 6.6. *Journal of Solid State Electrochemistry* **2004**, *8* (7), 497–504. https://doi.org/10.1007/s10008-004-0495-z.

(16) Gómez, E.; Pellicer, E.; Vallés, E. Influence of the Bath Composition and the PH on the Induced Cobalt–Molybdenum Electrodeposition. *Journal of Electroanalytical Chemistry* **2003**, *556*, 137–145. https://doi.org/10.1016/S0022-0728(03)00339-5.

(17) Kanani, N. *Electroplating: Basic Principles, Processes and Practice.*; Elsevier: Burlington, **2005.**

(18) Lasia, A. *Electrochemical Impedance Spectroscopy and Its Applications*; Springer New York: New York, NY, **2014.** https://doi.org/10.1007/978-1-4614-8933-7.

(19) Yuan, X.-Z.; Song, C.; Wang, H.; Zhang, J. *Electrochemical Impedance Spectroscopy in PEM Fuel Cells*; Springer London: London, **2010**. https://doi.org/10.1007/978-1-84882-846-9.